

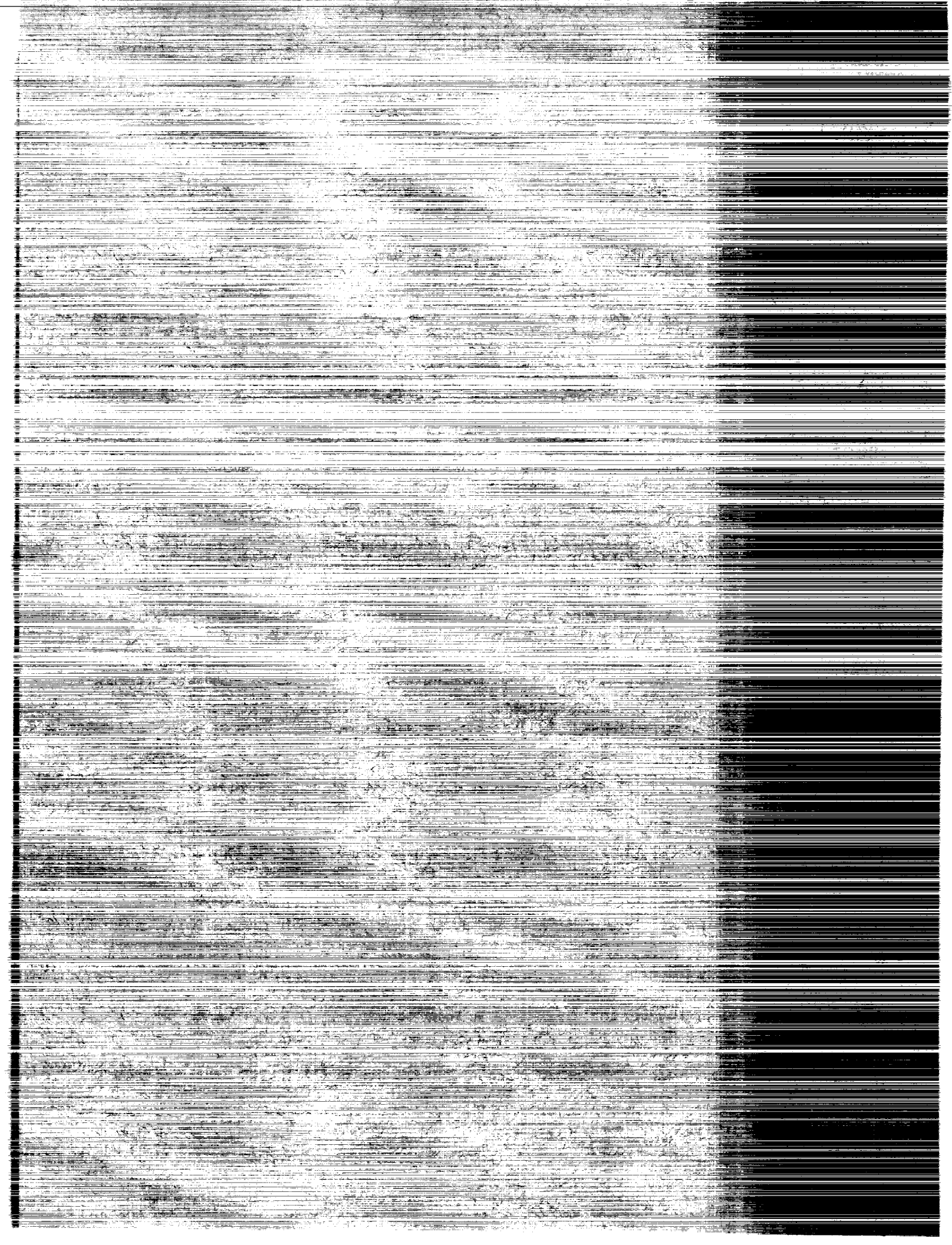
**NASA
Technical
Paper
2107**

January 1983

Modeling of Space Vehicle Propellant Mixing

John C. Aydelott

NASA



**NASA
Technical
Paper
2107**

1983

Modeling of Space Vehicle Propellant Mixing

John C. Aydelott
*Lewis Research Center
Cleveland, Ohio*

NASA
National Aeronautics
and Space Administration
**Scientific and Technical
Information Branch**



SUMMARY

An experimental program was conducted in the Lewis Research Center's zero-gravity facility to examine the liquid flow patterns that result from the axial-jet mixing of ethanol in 10-cm-diameter containers under zero-, reduced-, and normal-gravity conditions. Four tank configurations were used for this study: a spherical container; a convex hemispherically ended cylindrical container; and two Centaur liquid-hydrogen-tank models, one with slosh baffles and one without. Four distinct liquid flow patterns were observed: dissipation of the liquid jet in the bulk-liquid region, geyser formation, liquid collection at the end of the tank opposite the jet outlet, and complete circulation of the liquid along the tank walls. Dimensionless parameters were developed that characterized the liquid flow patterns and the bulk-liquid mixing phenomena.

INTRODUCTION

The use of cryogenic propellants in NASA's space program introduced problems of propellant management (ref. 1). During missions in space, cryogenic propellant tanks require periodic venting to keep the tank pressure within acceptable limits as a result of various heat inputs. Currently, orbiting propellant tanks are vented by using settling rockets to position and maintain the liquid away from the vent and thus to permit the venting of only vapor from the tank.

Efforts to improve the performance of propulsive stages have introduced the thermodynamic vent concept, a method of controlling tank pressure other than liquid settling and direct venting (ref. 2). Thermodynamic vent system concepts are particularly attractive when cryogenic payloads for the space shuttle are considered. Under many normal operating conditions and all abort modes, payload requirements cannot dictate shuttle operations, so settling to relieve the payload tank pressure would be impossible. Thermodynamic vent systems should impose no operating constraints on the space shuttle.

In the thermodynamic vent system a small amount of the cryogenic propellant is evaporated to offset the unavoidable heat addition to the propellant tank. Cryogenic liquid is withdrawn from the tank and passed through a Joule-Thompson valve with a resultant pressure and temperature reduction. This cold, two-phase fluid is then introduced into a heat exchanger, where evaporation continues and heat absorption takes place before the resulting vapor is vented overboard.

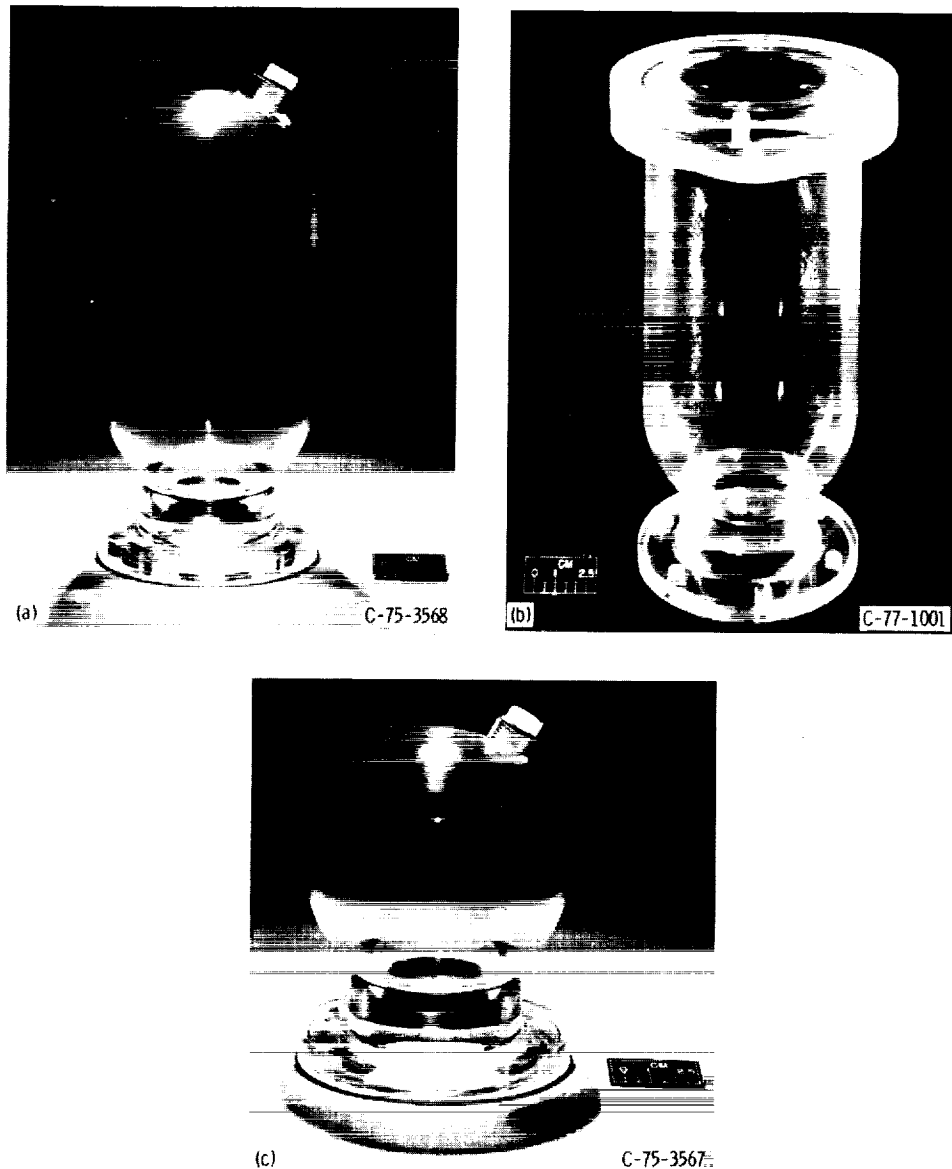
For large cryogenic tanks internal thermodynamic vent systems employing compact heat exchangers and fluid mixers are preferred because of their relatively low weight. However, the internal thermodynamic vent system introduces the requirement of circulating or mixing the fluid in the tank so that effective fluid cooling occurs and thus reduces the tank pressure.

Thermodynamic vent systems with internal, compact heat exchangers and mixers have been designed, fabricated, and tested in cryogenic fluids under normal-gravity conditions (ref. 3). The ability of these devices to control tank pressure at 1 g has led to their general acceptance as the planned pressure control technique for orbit transfer vehicles and other future cryogenic tankage designed for weightless operation.

Techniques for designing thermodynamic vent systems have not been verified experimentally under low-gravity conditions. Specifically, the design of the mixer is strongly influenced by the acceleration-dependent fluid

dynamics necessary to mix the tank contents in a predictable manner (refs. 4 and 5). The difference between normal gravity and weightlessness will influence not only the liquid-vapor configuration before mixing, but also the liquid momentum or velocity required to establish the desired liquid flow pattern and degree of mixing.

In earlier studies the author examined the liquid flow patterns that resulted when an axial liquid jet (a circular liquid jet directed along the axis of the container) was used to mix ethanol in 10-cm-diameter spherical (ref. 4) and cylindrical (ref. 5) containers (fig. 1) under weightlessness. Several tests were also conducted under normal-gravity conditions for comparison. The effects of the volume of liquid in the tank, the position of the liquid-jet outlet, and the liquid-jet flow rate on the resulting liquid flow patterns were examined. Reference 5 presents the author's rationale



(a) Cylindrical tank with convex hemispherical ends.

(b) Centaur liquid-hydrogen-tank model without slosh baffles.

(c) Spherical experiment tank.

Figure 1. - Experiment tanks.

for using axial liquid jets to provide fluid mixing and the criteria for selecting liquid-jet inflow rates.

The experimental program was continued by examining the liquid flow patterns that resulted when an axial liquid jet was used to mix the contents of partially filled spherical and cylindrical containers under reduced-gravity conditions. Acceleration levels were chosen that simulated the atmospheric drag that would exist on a full-scale propellant tank in low Earth orbit. Of equal importance with observing liquid flow patterns was examining the motion of the ullage, or main vapor region. Vapor encapsulation of the simulated pump (i.e., vapor ingested in the region of fluid withdrawal) would lead to failure of the liquid circulation concept.

The objectives of the program were (1) to determine how the acceleration environment, coupled with the previously studied range of variables, affects the resulting liquid flow patterns and (2) to establish analytical correlating parameters that would characterize the observed fluid dynamic phenomena.

SYMBOLS

a	acceleration, cm/sec ²
Bo	Bond number, $a\rho R_j^2/\sigma$
D	diameter, cm
F	flow characterization parameter, $(X + Y We)/(1 + Z Bo)$
G	ratio of geyser height to tank radius, h_g/R_t
g	acceleration due to gravity, 980 cm/sec ²
h	height, cm
M	mixing parameter, $Q\theta/V_b$
Q	liquid-jet volumetric inflow rate, cm ³ /sec
R	radius, cm
Re	Reynolds number, $\rho vD/\mu$
V	volume, cm ³
v	liquid-jet velocity, cm/sec
We	Weber number, $\rho v^2 R_0^2/\sigma D$
X,Y,Z	nondimensional constants
θ	bulk-liquid mixing time, sec
μ	viscosity, g/cm-sec

- ρ density, g/cm³
 σ surface tension, g/sec²

Subscripts:

- b bulk liquid
c completely turbulent
g geyser
j liquid jet
l laminar
o outlet
p partially turbulent
t tank or container

APPARATUS AND PROCEDURE

The Lewis zero-gravity facility was used to obtain the experimental data for this investigation. The facility, the experiment package, and the procedure for conducting the tests are described completely in the appendix of reference 5.

A schematic drawing of the liquid flow system is shown in figure 2. A piston pump, driven by an electric motor and gear mechanism, forces the ethanol test liquid out through the central tube and forms an axial liquid jet. Simultaneously, liquid is withdrawn from the bottom of the experiment tank and fills the region below the piston pumps. Interchangeable 0.4-cm-diameter liquid-jet outlet tubes of different lengths could be fit into the opening at the top of the piston pumps.

The speed of the piston pump, and thus the liquid-jet volumetric flow rate, is controlled by various combinations of gear drives and applied voltage to the electric motor. As the piston moves, an electrical contact slides along a linear resistor mounted parallel to the piston pump. A 28-V, direct-current circuit, including the linear resistor that acts as a voltage divider, provides the input to a telemetry system that transmits to a receiver and a strip-chart recorder in the facility control room so that the position of the piston pump as a function of time can be determined. Because the piston drive mechanism occupies approximately 30 percent of the piston sleeve volume, the liquid volumetric withdrawal rate is only 70 percent of the liquid-jet volumetric flow rate.

During a test under zero- or reduced-gravity conditions the first 2 sec of test time was allocated for the bulk liquid to achieve a reduced- or zero-gravity configuration. The liquid flow system was then activated by timers for the remaining test time, 3.1 sec. For simplicity, the same sequence and timing of operations were used for the normal-gravity tests.

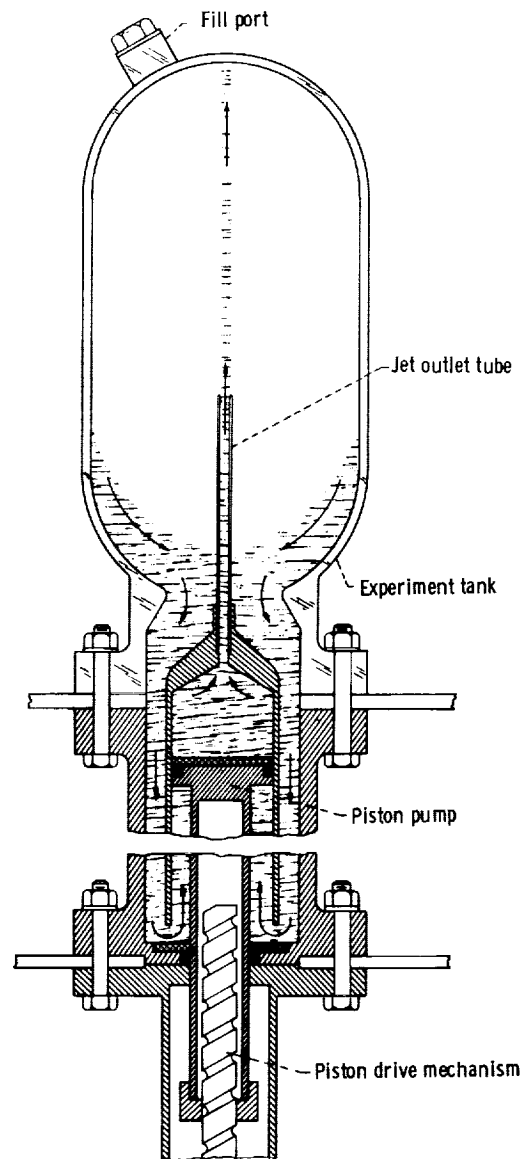


Figure 2. - Liquid flow system.

A high-speed motion picture camera was used to photograph the initial bulk-liquid motion and the liquid flow patterns within the experiment tanks after the piston pump was activated. The liquid jet was dyed to clarify the liquid flow patterns. A digital clock was included in the camera field of view so that the elapsed time from the start of the test would be recorded.

Four 10-cm-diameter experiment tank configurations were used for the study. The four tanks are identified in table I by the following letters: A - convex hemispherically ended cylindrical tank with a length-diameter ratio of 2 and a volume of 1310 cm³; B - a Centaur liquid-hydrogen-tank model with one convex hemispherical end, one concave ellipsoidal end, no slosh baffles, a length-diameter ratio of 2, and a volume of 1270 cm³; C - a similar Centaur liquid-hydrogen-tank model that included internal slosh baffles at the 30- and 77-percent liquid fill levels; and D - a spherical tank with a volume of 524 cm³.

The piston pump was located in the convex hemispherical end of each tank. This location provided simulation of the liquid flow patterns

TABLE I. - SUMMARY OF TEST CONDITIONS AND ANALYTICAL RESULTS

Test	Tank shape	Acceleration, g's	Liquid filling, vol %	Jet outlet tube length, cm	Jet flow rate, Q , cm^3/sec	Jet Reynolds number, Re	Liquid height above jet outlet, h_b , cm	Jet Weber number, We	Jet Bond number, Bo	Liquid flow pattern	Ratio of Geyser height to tank radius, G	Flow characterization parameter, F	Liquid bulk mixing time, θ , sec	Mixing parameter, M
1	C	0	29	1	3.0	630	5.6	0.96	0	I/II	0.55	0.79	5.9	0.070
2	C	0	29	1	4.3	900	5.6	1.09	0	↓	.80	.68	5.0	.054
3	A	.0050	31	1	4.3	900	6.0	1.02	.11	↓	.69	.66	7.1	.074
4	A	.0095	32	1	4.3	900	5.9	1.04	.20	III	.52	2.11	---	---
5	C	0	29	1	6.2	1320	5.6	1.63	0	III	2.10	---	---	---
6	A	.0050	30	1	6.0	1290	5.8	1.51	.22	II	2.04	1.69	---	---
7	A	.0099	32	1	6.3	1320	5.9	1.55	.45	II	1.20	1.56	---	---
8	A	.014	31	1	6.1	1290	5.9	1.48	.63	I/II	.86	1.36	---	---
9	B	0	29	1	8.6	1820	3.1	5.51	0	IV	---	8.32	---	---
10	A	.0095	31	1	8.5	1800	5.8	2.91	.42	IV	---	3.32	---	---
11	A	.014	31	1	8.5	1800	6.0	2.81	.66	II	2.40	2.86	---	---
12	B	0	39	1	2.1	450	5.5	.49	0	I	.36	---	---	---
13	B	0	39	1	4.3	900	5.5	1.11	0	I/II	.84	.81	6.5	.057
14	B	0	38	1	6.1	1290	5.5	1.59	0	II/III	2.16	2.04	---	---
15	C	0	50	1	2.1	450	8.1	.39	0	I/II	.42	---	---	---
16	C	1	52	1	2.1	450	8.8	.37	10.6	I	---	---	---	---
17	C	0	51	1	3.0	630	8.1	.78	0	I	.34	---	---	---
18	A	0	52	8	3.0	630	1.4	2.04	0	III	2.40	---	---	---
19	C	0	52	1	4.3	900	7.6	.81	0	I/II	.52	.51	---	---
20	A	.0045	50	1	4.3	900	9.5	.65	.25	I	.30	.30	16.0	.102
21	A	1	52	1	6.3	1320	9.2	.67	.47	I	.32	.29	13.6	.087
22	C	0	52	1	6.2	1320	8.8	.70	47	I	---	.014	6.9	.045
23	A	0	52	8	6.3	1320	1.5	4.08	0	IV	---	---	---	---
24	A	0	52	1	6.3	1320	7.9	1.16	0	II	1.45	1.36	11.5	.115
25	A	.0045	52	1	6.2	1320	9.5	.97	.52	I/II	.94	.80	7.1	.069
26	A	.0090	54	1	6.8	1430	9.1	1.18	.96	I/II	.80	.88	7.4	.076
27	C	.014	52	1	6.2	1320	9.3	.99	1.55	I/II	.50	.56	9.9	.094
28	C	1	51	1	6.1	1290	8.8	1.00	100	I	---	.018	5.3	.050
29	A	0	50	8	6.1	1290	1.9	8.48	0	IV	---	---	---	---
30	A	0	52	1	8.8	1840	8.3	2.14	0	IV	---	2.92	---	---
31	A	.0092	53	1	8.7	1820	9.3	1.88	1.02	II	1.50	1.56	8.8	.124
32	A	.014	51	1	8.7	1820	9.4	1.86	1.59	II	1.30	1.27	5.1	.073
33	B	1	52	1	8.5	1800	8.9	1.91	102	I	---	.041	4.4	.057
34	A	0	53	8	8.9	1870	2.0	17.8	0	IV	---	---	---	---
35	A	0	55	1	12.5	2640	8.1	4.52	0	IV	---	6.73	4.8	.112
36	A	1	52	1	12.5	2640	9.2	3.99	109	I	---	.089	3.6	.066
37	A	0	49	8	11.5	2430	1.4	29.9	0	IV	---	---	---	---
38	A	0	52	8	11.5	2430	2.2	29.9	0	(a)	---	---	---	---
39	A	1	52	8	16.8	3540	7.3	9.01	---	IV	---	13.9	3.7	.118
40	B	1	51	1	17.1	3620	8.8	7.83	99.5	I	.24	.20	3.2	.086
41	A	0	52	8	16.6	3510	1.4	62.5	0	IV	---	---	8.2	---
42	A	0	52	1	23.4	4940	7.9	16.2	0	IV	---	---	3.1	(b)
43	A	0	52	1	24.2	5120	9.1	15.2	106	I/II	.40	25.4	2.0	.073
44	A	0	52	8	24.4	5150	1.3	134	0	IV	---	.37	6.7	---
45	A	1	52	8	24.4	5150	2.2	134	---	(a)	---	---	---	---

a Fountain.
b Recirculation.
c Bubbles.

TABLE I. - CONCLUDED

Test	Tank shape	Acceleration, g's	Liquid filling, vol %	Jet outlet tube length, cm	Jet flow rate, Q, cm ³ /sec	Jet Reynolds number, Re	Liquid height above jet outlet, h _j , cm	Jet Weber number, We	Jet Bond number, Bo	Liquid flow pattern	Ratio of Geyser height to tank radius, G	Flow characterization parameter, F	Liquid bulk mixing time, θ, sec	Mixing parameter, M
46	A	0	52	1	35.4	7470	7.8	37.6	0	IV	0.78	59.7	(b), (c)	0.077
47	↓	1	52	1	35.4	↓	9.1	32.3	106	I/II	---	.79	1.4	---
48	↓	0	51	8	35.4	↓	7.7	283	0	IV	---	---	(b), (c)	---
49	↓	1	52	8	35.4	↓	2.1	125	7.1	IV	---	37.9	(c)	---
50	B	0	60	1	2.1	450	8.9	.37	0	I	.24	---	---	---
51	↓	0	60	1	4.3	900	8.6	.72	0	I/II	.42	0.42	12.3	.070
52	↓	0	60	1	6.2	1320	8.7	1.05	0	I/II	1.10	1.18	9.9	.086
53	↓	0	73	↓	4.3	900	10.9	.57	0	I	.30	.27	17.9	.083
54	A	-0.020	74	↓	4.3	900	12.1	.51	.18	I	.20	.19	14.7	.066
55	A	-0.048	74	↓	4.2	880	12.2	.48	.43	I	.20	.14	15.1	.066
56	A	-0.046	74	8	4.4	920	6.3	1.92	.03	II/III	2.40	---	---	---
57	B	0	73	1	6.0	1270	10.9	.78	0	I/II	.70	.75	11.3	.077
58	A	-0.022	74	1	6.3	1320	12.4	.74	.43	I/II	.50	.54	9.9	.068
59	A	-0.043	73	1	6.0	1270	12.2	.70	.82	I/II	.50	.41	13.7	.089
60	B	0	73	1	8.5	1800	10.9	1.56	0	IV	---	2.00	---	---
61	A	-0.096	76	↓	8.5	1800	12.9	1.32	2.04	I/II	1.04	.72	7.9	.072
62	A	-0.14	73	↓	8.6	1820	12.7	1.38	2.88	I/II	.76	.63	8.2	.077
63	A	.014	76	8	8.8	1850	5.9	3.03	.63	IV	---	3.16	9.8	.092
64	B	0	91	1	2.2	480	13.3	.31	0	I	.10	---	---	---
65	C	↓	91	1	4.3	900	13.0	.48	↓	I	.20	.18	---	---
66	C	↓	92	↓	6.1	1290	14.2	.62	↓	I/II	.48	.49	---	---
67	B	↓	92	↓	8.5	1800	12.8	1.33	↓	IV	---	1.63	---	---
68	D	↓	30	↓	4.3	900	.6	4.08	---	(a)	---	---	---	---
69	↓	1	30	↓	4.3	900	2.6	2.28	0	IV	---	---	---	---
70	↓	0	29	↓	6.1	1290	.7	8.48	0	IV	---	---	---	---
71	↓	-0.042	27	↓	6.1	1290	2.6	3.29	.04	IV	---	4.65	---	---
72	↓	-0.090	27	↓	6.0	1270	2.8	2.94	.10	IV	---	3.97	---	---
73	↓	-0.090	49	↓	4.3	900	4.1	1.48	.10	II/IV	1.00	1.11	---	---
74	↓	-0.014	49	↓	4.3	900	3.9	1.55	.13	II	.94	1.16	---	---
75	↓	0	50	↓	6.0	1270	.8	8.14	0	IV	---	---	---	---
76	↓	-0.040	49	↓	↓	↓	3.6	2.31	.07	IV	---	3.07	4.0	.101
77	↓	-0.090	47	↓	↓	↓	4.1	2.03	.20	IV	---	2.45	---	---
78	↓	1	48	↓	↓	↓	3.9	2.13	20.2	I	.23	.22	---	---
79	↓	-0.090	69	↓	4.3	900	5.4	1.13	.16	I/II	.48	.76	3.6	.043
80	↓	-0.014	68	↓	4.3	900	5.2	1.17	.24	I/II	.45	.76	5.2	.064
81	↓	0	72	↓	6.1	1290	1.3	8.48	0	(d)	---	---	---	---
82	↓	-0.044	69	↓	6.0	1270	5.0	1.68	.14	II/IV	.80	2.02	---	---
83	↓	0	69	↓	6.0	1270	---	8.14	---	(d)	---	---	---	---
84	↓	-0.045	69	↓	6.0	1270	---	8.14	---	IV	---	---	7.8	---
85	↓	-0.085	89	↓	4.3	900	6.5	.94	.22	I/II	.36	.57	---	---
86	↓	-0.14	89	↓	4.3	900	6.8	.90	.40	I/II	.38	.48	7.0	.065
87	↓	0	87	↓	6.2	1320	1.3	8.83	0	(e)	---	---	---	---
88	↓	-0.042	91	↓	6.0	1270	6.3	1.34	.22	II/III	.70	1.45	5.1	.071
89	↓	0	88	↓	6.0	1270	---	8.14	---	(e)	---	---	---	---
90	↓	-0.047	88	↓	6.0	1270	---	8.14	---	IV	---	---	---	---
91	↓	1	88	↓	12.0	2530	6.8	4.96	59.9	I	.21	.20	---	---

a. Fountain, b. recirculation, c. bubbles, d. liquid collection on side walls, e. vapor encapsulation of pump.

associated with a pump in the forward end of each tank. The forward end of the tank was chosen as the pump location because under Earth-orbiting conditions liquid would be positioned over the pump as a result of the acceleration caused by atmospheric drag.

For this experimental study, tank Bond numbers (acceleration to surface tension force ratio) of 2, 4, 8, and 12 were chosen to cover the range of accelerations expected on orbit transfer vehicle propellant tanks. These Bond numbers correspond to accelerations on the experiment package of 0.0023, 0.0046, 0.0092, and 0.014 g's, which were achieved by the use of a cold gas thruster. Other experimental variables were initial experiment tank liquid filling, axial liquid-jet outlet position, and liquid-jet volumetric flow rate.

The lengths of the axial jet outlet tubes, 1 and 8 cm, were measured from the hypothetical bottom of each experiment tank. For each test the average piston pump velocity was determined from the position-versus-time trace obtained from the strip-chart recorder. The average piston pump velocity was multiplied by the piston cross-sectional area to obtain the liquid-jet volumetric flow rate.

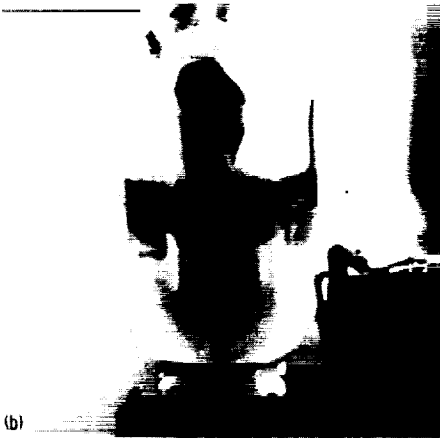
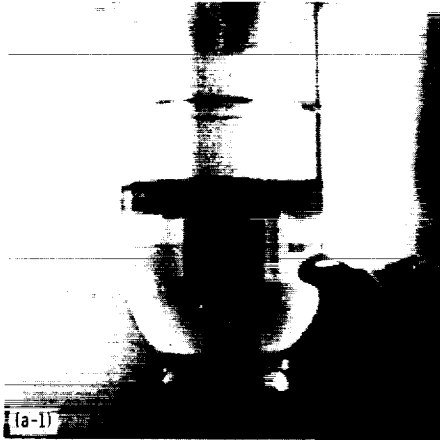
EXPERIMENTAL RESULTS

The experimental conditions for the 14 normal-gravity tests, 36 reduced-gravity tests, and 41 zero-gravity tests ($<10^{-5}$ g's), together with the characteristics of the axial liquid jet for each test, are presented in table I. The data from all of the reduced-gravity tests and those from the zero-gravity tests with initial experiment-tank liquid fillings of approximately 40 and 60 percent (by volume) have not been previously published; the remaining data are taken from references 4 and 5 for comparison.

Four distinct liquid flow patterns, previously observed and discussed in reference 5, are shown in figure 3 and identified by the following Roman numerals in table I: I - dissipation of the liquid jet in the bulk-liquid region (fig. 3(a)), II - geyser formation (fig. 3(b)), III - collection of jet liquid in the aft end of the tank (opposite the jet outlet) (fig. 3(c)), IV - liquid circulation over the aft end of the tank and down the tank wall (fig. 3(d)).

Many of the tests exhibited results that combined characteristics of two flow patterns. Experimental conditions that produced some bulk-liquid mixing together with the formation of fairly prominent geysers are identified by the Roman numerals I/II. Tests identified as having flow patterns II/III or II/IV indicate the author's uncertainty due to the limited test time. A few tests that resulted in liquid flow patterns that do not fall into any of the previously discussed categories are identified by footnotes.

The liquid height above the liquid-jet outlet was measured just prior to the movement of the piston pump. The maximum height of each geyser was also measured and divided by the tank radius. The time required, after the piston pump began to move, for complete bulk-liquid mixing was either measured or extrapolated from the data for each test. The measured bulk-liquid mixing times are the times required for the bulk liquid to become completely dyed by the incoming liquid jet. The shortcomings associated with the use of a dyed liquid jet in an isothermal system to simulate the mixing of nonisothermal liquids are examined in the section Concluding Remarks. The extrapolation technique involved measuring the position of the demarcation line between the dyed and undyed liquids in the bulk-liquid region as a function of time. From these measurements the velocity of the demarcation



(a-1) Normal gravity, test 16. (a-2) Weightlessness, test 17.
(a) Dissipation of liquid jet in bulk-liquid region.
(b) Geyser formation, test 24.
(c) Liquid collection, test 18.
(d) Liquid circulation, test 42.

Figure 3. - Observed axial liquid-jet flow patterns.

line between the dyed and undyed liquids was determined and multiplied by the tank cross-sectional area to establish the bulk-liquid mixing rate. The volume of unmixed liquid bulk at the end of each test was then divided by this experimentally determined mixing rate, and the resulting time increment was added to the test time to obtain an estimate of the time required for complete bulk mixing. Tests for which bulk-liquid mixing times are not presented fall into three categories:

(1) Low liquid-jet flow rates coupled with only 3 sec of test time yield immeasurable rates of bulk-liquid mixing (flow patterns I and IV).

(2) Mixing of the liquid jet and the bulk liquid is negligible (flow patterns II and III).

(3) Bulk-liquid mixing phenomena are affected by the presence of slosh baffles.

ANALYSIS OF EXPERIMENTAL RESULTS

Dimensional Analysis of Liquid-Jet Flow Patterns

Studies of liquid inflow to model tanks under reduced-gravity conditions (refs. 6 and 7) provided the basis for the author's analysis of the experimental data presented herein. The height of the liquid geyser that forms during inflow was selected as the most prominent physical characteristic of the observed fluid dynamic phenomena. The geyser height is also a suitable physical characteristic to describe three of the four flow patterns that were observed during the propellant mixing studies: flow pattern I is distinguished by negligible geyser heights, flow pattern II is described directly by geyser height, and flow pattern III is characterized by geysers that just touch the aft end of the tank opposite the jet outlet.

The inertia, acceleration, and surface tension forces are the primary factors that determine geyser formation. Examination of the formulas that describe these forces leads to the selection of the liquid-jet velocity, density, and surface tension, the acceleration, the geyser height, and several characteristic dimensions as the important parameters in this study.

The Buckingham theorem was employed to establish three dimensionless groups that can be used to correlate the experimental data: the Bond Bo and Weber We numbers and a nondimensional geyser height G . The Bond number is the ratio of acceleration to surface tension forces, and the Weber number is the ratio of inertial to surface tension forces. To avoid confusion, the reader should recognize the difference between the liquid jet Bond number and the tank Bond number. The liquid-jet Bond number, based on the jet radius R_j , is used to characterize the interaction between the liquid jet and the liquid-vapor interface. The tank Bond number, based on the tank radius R_t , is used to characterize the bulk-liquid behavior.

The three dimensionless groups are

$$G = h_g/R_t \quad (1)$$

$$Bo = a\rho R_j^2/\sigma \quad (2)$$

$$We = \rho v_0^2 R_0^2 / \sigma D_j \quad (3)$$

With one exception the parameters contained in these three dimensionless groups are either fluid properties, easily measured dimensions, or terms that can be readily calculated by using the continuity equation. Establishing the functional relationship between the experimental variables and the radius of the liquid jet proved to be a significant portion of the analytical effort.

Axial liquid-jet physical characteristics. - The velocity with which the liquid jet exits the simulated pump affects not only the momentum of the jet and thus the resulting liquid flow pattern, but also the physical appearance or characteristics of the liquid jet (ref. 8). At very low velocities the liquid jet is laminar, with almost undetectable spreading of the jet as it passes through the bulk liquid (fig. 3(a-1)). As the liquid jet velocity is increased, a transition to completely turbulent flow occurs, and the jet spreads into the bulk region at an angle of up to 12° on each side of the jet centerline (fig. 3(b)).

Because of the liquid-jet spreading phenomenon, the position of the outlet for an axial liquid jet relative to the bulk liquid-vapor interface greatly affects the resulting jet characteristics. According to the classical theory for the behavior of axial jets flowing through a fluid (ref. 9), a submerged jet maintains nearly constant momentum as it progresses from the outlet. As the jet flows through the bulk liquid, its mass flow rate increases because of bulk-liquid entrainment, and its average velocity decreases because of radial momentum transport by viscous effects. Consequently, for axial jets with outlets positioned in the bulk liquid, increasing the liquid depth over the axial liquid-jet outlet will increase the size and mass flow rate of the liquid jet and reduce its average velocity at the liquid-vapor interface. Comparison of figures 3(b) and (c) provides dramatic evidence of this fluid dynamic phenomenon.

The jet outlet position and tank filling are not the only parameters that determine the depth of bulk liquid that the liquid jet must penetrate. Under weightless conditions the liquid-vapor interface becomes hemispherical, and thus liquid depth over the jet outlet is less than with the same tank filling under normal gravity. Two exceptions to this occur in the baffled Centaur model tank. For tank liquid fillings of approximately 30 and 70 percent the lower and upper slosh baffles, respectively, restrict the motion of the liquid-vapor interface so that the highly curved zero-gravity configuration typical of unbaffled tanks does not occur. Consequently, the liquid depth over the jet outlet was greater for these test conditions than for the corresponding tests in the unbaffled tanks.

Correlation of liquid-jet characteristics. - Reference 6, which presents a summary of the pertinent literature, suggests that, at liquid-jet Reynolds numbers greater than approximately 1500, the jet should be completely turbulent. The following form of the Reynolds number was used for this study:

$$Re = \rho v_0 D_0 / \mu \quad (4)$$

The calculated value of the Reynolds number for each experimental test can be found in table I.

A completely turbulent jet should be expected to spread to about 6° to 8° on each side of the jet centerline for a distance of 12.4 jet outlet radii and then to about 10° to 12° for greater distances. From these angles of spread, the following approximate expressions for the radius of the liquid jet can be derived (ref. 6), where h_b is the distance between the jet outlet and the liquid-vapor interface:

$$R_{j,c} = R_o + 0.12 h_b \quad h_b \leq 12.4 R_o \quad (5)$$

$$R_{j,c} = 0.11 R_o + 0.19 h_b \quad h_b > 12.4 R_o \quad (6)$$

For laminar liquid jets the angle of spread is only 2° to 3° on either side of the jet centerline. For these conditions of jet spreading the approximate expression for the radius of the liquid jet as a function of the liquid height above the liquid-jet outlet is

$$R_{j,l} = R_o + 0.04 h_b \quad (7)$$

The angle of spread of the liquid jet, based on measurement of the penetration of the dyed fluid into the bulk-liquid region, was determined for each experimental test. Comparison of the experimentally obtained measurements of the liquid-jet dimensions with the previously presented theory led to the following conclusions:

(1) For experimental conditions that yielded Reynolds numbers in excess of 1250 and liquid heights above the liquid-jet outlet greater than 2.5 cm ($12.4 R_o$), agreement between equation (6) and the experimental results was good.

(2) The data obtained at a liquid-jet Reynolds number of 630 and liquid heights greater than 2.5 cm agreed almost exactly with equation (7).

(3) At liquid-jet Reynolds numbers of approximately 450 no spreading of the jet could be measured.

(4) When the liquid-jet outlet was less than 2.5 cm below the liquid-vapor interface, the resulting jet had the same radius as the jet outlet tube. This experimental observation conflicts with the predictions of equation (5); the reason for the difference could not be determined.

(5) For experimental conditions that yielded Reynolds numbers of approximately 900 and liquid heights greater than 2.5 cm, the liquid-jet characteristics were intermediate between the laminar and completely turbulent results. The following equation was found to fit the experimental data for these conditions:

$$R_{j,p} = 0.10 R_o + 0.13 h_b \quad h_b > 12.4 R_o \quad (8)$$

The preceding criteria were used to determine the liquid-jet radii at the liquid-vapor interface for each test. Then, by using equations (2) and (3), the liquid-jet Weber and Bond numbers were calculated and recorded in table I.

In addition, for those tests that resulted in flow pattern II, III, or IV, the width of the geyser was measured just above the liquid-vapor interface. Examination of these data led to the following conclusions:

(1) When the liquid-jet outlet was less than 2.5 cm below the liquid-vapor interface, no dissipation of the liquid jet in the bulk liquid was apparent, and the resulting geyser had the same radius as the jet outlet tube.

(2) For liquid heights above the liquid-jet outlet greater than 2.5 cm, the radius of the resulting geyser was 10 to 20 percent smaller than the radius of the liquid jet at the liquid-vapor interface. This observation can be explained by realizing that the geyser is formed from the higher velocity central core of the liquid jet while the lower velocity outer extremities of the jet are dissipated in the bulk liquid.

Correlation of liquid-jet dimensionless groups. - To establish the functional relationship between the three dimensionless groups established by the Buckingham theorem, all of the partially turbulent (Reynolds number, approx 900) zero-gravity cylindrical tank data were examined. This initial screening, which included only zero Bond number data, led to the conclusion that a linear functional relationship exists between the nondimensional geyser height and the liquid-jet Weber number:

$$G = f(X + Y We) \quad (9)$$

The logical assumptions that the geyser height should be inversely proportional to the magnitude of the acceleration environment and that the correlating expression must reduce to equation (9) under zero-gravity conditions yield

$$G = f\left(\frac{X + Y We}{1 + Z Bo}\right) \quad (10)$$

Use of a least-squares deviation curve-fitting technique for the partially turbulent zero-gravity experimental data established values for the constants X and Y of -0.3 and 1.0, respectively. The negative value for X reflects the fact that a finite jet velocity and corresponding Weber number are required before the liquid jet is not totally dissipated in the liquid bulk and a geyser forms. Further curve fitting of the reduced- and normal-gravity data established a value of 0.6 for the constant Z. Thus a flow characterization parameter F_p was established that can be used to describe the flow patterns resulting from partially turbulent ($h_b > 2.5$ cm) submerged liquid jets with Reynolds numbers of approximately 900:

$$F_p = \frac{We - 0.3}{1 + 0.6 Bo} \quad (11)$$

Figure 4(a) shows the excellent correlation that was achieved between the experimentally determined nondimensional geyser heights and the calculated flow characterization parameters for the partially turbulent liquid jets.

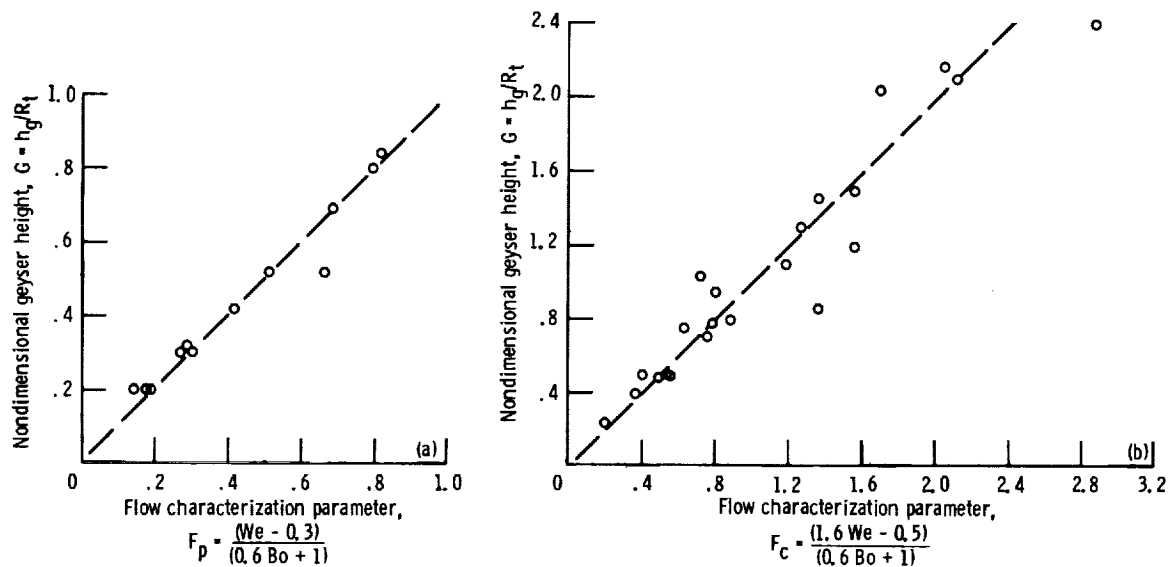
A correlating equation was similarly derived for completely turbulent (Re > 1250) submerged liquid jets:

$$F_c = \frac{1.6 We - 0.5}{1 + 0.6 Bo} \quad (12)$$

Figure 4(b) is a plot of the experimentally determined nondimensional geyser height versus the flow characterization parameter for the completely turbulent liquid jets. The data scatter exhibited by this figure, as compared with figure 4(a), should be expected based on the wide range of flow rates that are included in the turbulent liquid-jet data. Also, the starting points for this analysis, reference 6 and equations (5) and (6), were established based on steady-state experimental conditions for a gas jet flowing into a gaseous environment. Although gas-gas and liquid-liquid systems should exhibit similar characteristics (ref. 9), the short test times associated with this experimental study suggest that transient effects could also contribute to the observed data scatter.

Values of the flow characterization parameter for both the partially and completely turbulent liquid jets are recorded in table I. Because of the limited amount of laminar liquid-jet data no attempt was made to correlate the experimental results for these test conditions. However, a comparison of the Weber numbers and the nondimensional geyser heights for the laminar liquid-jet tests indicates that the same general functional relationship exists. For the test conditions where the liquid jets exited near the liquid-vapor interface ($h_b < 2.5$ cm), only flow patterns III and IV resulted under zero- or reduced-gravity conditions. Consequently, no correlation of the experimental results was possible since the geysers or jets are constrained by the test container and their maximum height cannot be determined.

Flow characterization parameters were also calculated by using equations (11) and (12) for the tests conducted in spherical containers (table I). Although the same general trends exist, good agreement between



(a) Jet Reynolds number, $Re_j \approx 900$.

(b) Jet Reynolds number, $Re_j > 1250$.

Figure 4 - Nondimensional geyser height as a function of flow characterization parameter. Cylindrical tank data only.

the experimentally determined nondimensional geyser height and the corresponding values of the flow characterization parameter did not result; a possible explanation for this variance is presented in the section Discussion of Results.

Bulk-Liquid Mixing Correlation

References 10 and 11, which present an extensive review and summarization of fluid mixing theory, were the sources of several liquid-mixing correlating parameters. Values of these correlating parameters were calculated for the test results reported herein for which bulk-liquid mixing times and flow characterization parameters had been determined. A mixing correlation parameter $\theta Q h_b^{1/2} D_t^{1/2} / V_t D_j$ originally developed by Okita and Oyama (ref. 12) was found to be a function of the flow characterization parameters over a wide range of experimental variables. Since the work of Okita and Oyama dealt only with completely filled tanks, the bulk-liquid volume V_b was substituted for the tank volume V_t to account for the variation in the liquid filling that was one of the variables in this experimental program. In addition, the characteristic dimensions contained in the reference 12 mixing parameter were either constants ($D_t^{1/2}$ and D_j) or varied only slightly ($h_b^{1/2}$) in this experimental program. Consequently, the Okita and Oyama mixing parameter was reduced to a much simpler form - the liquid-jet volumetric flow rate divided by the bulk-liquid mixing rate:

$$M = \frac{Q}{V_b / \theta} \quad (13)$$

In this expression the liquid-jet volumetric flow rate Q is an independent variable. The bulk-liquid volume V_b is dependent on both the initial tank filling and the liquid-jet characteristics. The bulk-liquid mixing time θ is a dependent variable whose values were determined experimentally. To make the experimental results more useful, an analytical technique was developed that provides a means of determining approximate values for the bulk-liquid volumes.

The volume of liquid initially in the experiment tanks is reduced by the action of the liquid jets through the formation of geysers (flow patterns II, III, and IV) and the presence of liquid on the tank walls in the end of the tank opposite the mixer unit (flow patterns III and IV). Since no bulk-liquid mixing was observed for test conditions that yielded flow pattern III, the analysis was restricted to examination of flow patterns II and IV.

For test conditions that produce only geysers the bulk-liquid volume can be determined by subtracting the volume of liquid in the geyser from the initial volume of liquid in the experiment tanks; the difference between the liquid-jet volumetric flow rate and the rate of liquid withdrawal at the base of the simulated mixer unit is small and was neglected. The volume of liquid in the geysers can be approximated by using the previously presented analytical techniques. On the basis of the liquid jet Reynolds number the appropriate equations for the liquid-jet radius at the liquid-vapor interface, equation (6) or (8), and for the nondimensional geyser height,

equation (11) or (12), can be employed to calculate the bulk-liquid volume (flow pattern II):

$$V_b = V_t (\% \text{ filling}) - \pi R_j^2 F R_t \quad (14)$$

For test conditions that produce flow pattern IV both the volume of liquid in the geyser and the volume on the tank walls must be subtracted from the initial volume of liquid in the experiment tank to establish the bulk-liquid volume. The geyser radius is once again approximated by using either equation (6) or (8), and the geyser height is now the distance from the liquid-vapor interface to the end of the tank opposite the mixer unit:

$$h_g = h_t - h_b - h_o \quad (15)$$

Analytical techniques originally developed by Prandtl and subsequently experimentally verified (ref. 13) indicate that liquid jets which impinge on a solid surface can be characterized as having uniform and continuous velocity profiles. The only exceptions to this general observation occur in the thin boundary layer of fluid adjacent to the tank wall and in the immediate vicinity of the point of impingement of the liquid jet. Consequently, for the engineering solution required by this analysis, it is possible to neglect the boundary layer and jet impingement point effects and to assume that the average velocity of each geyser is equal to the resulting average velocity of the liquid flowing on the tank walls. This assumption is reasonably applied only to the hemispherically ended tanks (tank shapes A and D). However, this restriction is of no consequence since no bulk-liquid mixing times were established for experimental conditions that yielded flow pattern IV in the Centaur model tanks (tank shapes B and C). Because continuity must be preserved as the liquid flows on the tank wall, the cross-sectional area of this liquid is constant and only the thickness of the liquid changes to accommodate the geometry of the tank. For tank shapes A and D a simple geometric analysis yields the following expression for the bulk-liquid volume (flow pattern IV):

$$V_b = V_t (\% \text{ filling}) - \pi R_j^2 \left[2h_g + R_t \left(\frac{\pi}{2} - 1 \right) - R_j \right] \quad (16)$$

The values of the mixing parameter M (eq. (13)) calculated by using bulk-liquid volumes determined from equation (14) (flow pattern II) or equation (16) (flow pattern IV) can be found in table I.

Figure 5 presents a plot of the mixing parameter as a function of the flow characterization parameters for the data obtained in the cylindrical tanks with a jet outlet tube 1 cm long. The data obtained with partially turbulent liquid jets generally exhibited more scatter than data for completely turbulent liquid jets. This observation can be explained by realizing that the partially turbulent liquid jets result from relatively low liquid-jet flow rates. Because of the limited test time available, low liquid-jet flow rates yield the least observed quantity of bulk-liquid mixing and thus the greatest extrapolation of the experimental data.

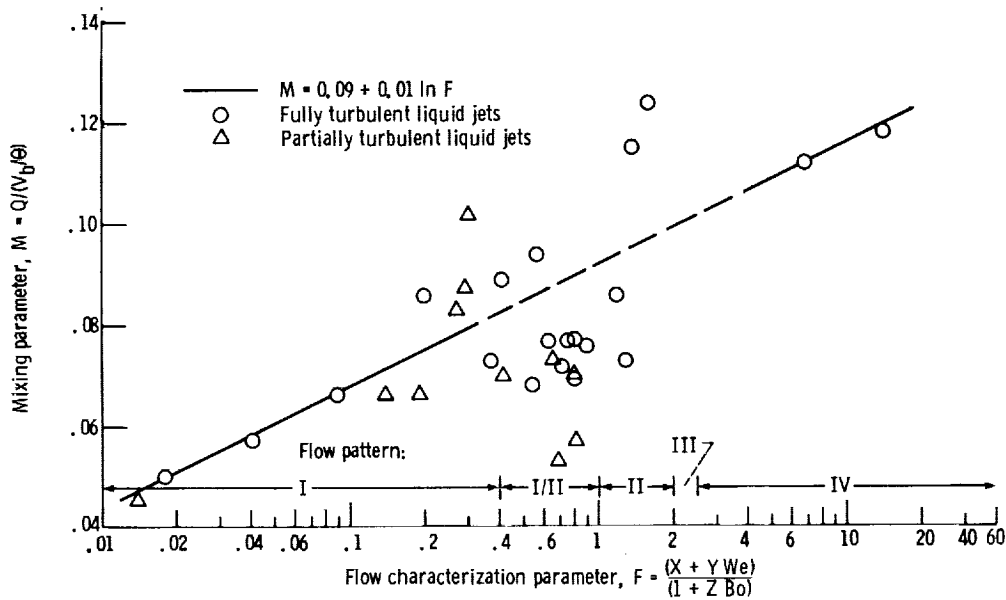


Figure 5. - Mixing parameter as a function of flow characterization parameter. Cylindrical tanks with 1-cm jet outlet tubes.

For experimental conditions that yield liquid flow patterns I and IV, the mixing parameter increases steadily as the flow characterization parameter increases. Although these flow patterns are strikingly different, the resulting bulk-liquid mixing phenomena are both observationally and analytically similar. The following functional relationship exists between the mixing and flow characterization parameters for liquid flow patterns I and IV:

$$M = 0.09 + 0.01 \ln F \quad (17)$$

In the transition region from flow pattern I to flow pattern II, there is a lot of scatter in the values of the mixing parameter. This data scatter could be anticipated from observing the flow phenomena, which exhibit a great deal of irregular flow and a pulsing motion of the geysers that form. This pulsing motion aids bulk-liquid mixing so that the mixing parameter decreases in value as the flow characterization parameter increases. As the flow characterization parameter increases to the point where large geysers result (flow pattern II), the bulk-liquid mixing times are longer because mixing is negligible. For experimental conditions that yield flow pattern III, no bulk-liquid mixing occurs and the value of the mixing parameter approaches infinity.

Values of the mixing parameter were also calculated for the experimental tests conducted in the spherical tanks and for the one test (no. 63) that was conducted in a cylindrical tank with an 8-cm-long liquid-jet outlet tube. The same general trends in the functional relationship between the mixing parameter and the flow characterization parameter were observed for these data. However, the mixing parameters were generally lower at the same flow conditions. Because of the uncertainty in the validity of applying the flow-characterization-parameter calculation procedure for the 1-cm-long-liquid-jet-outlet-tube cylindrical tank to the spherical tank and test 63 data, these mixing data were not plotted in figure 5.

DISCUSSION OF RESULTS

A few data points included in table I exhibited liquid-jet flow characteristics and bulk-liquid mixing phenomena that do not fit into the general categories introduced in the previous sections.

Test 56 was the only data point obtained for both an 8-cm-long outlet tube and appreciable liquid depth at a jet Reynolds number of approximately 900. Observation of the penetration of the liquid-jet dye into the bulk liquid revealed a thin laminar jet similar to the liquid jets that resulted at lower Reynolds numbers with the 1-cm-long outlet tube. It is the author's opinion that the longer jet outlet tube yields a more completely developed liquid-jet velocity profile and that the transition to partially turbulent flow thus does not occur. Consequently, the Weber and Bond numbers for test 56 were calculated by using equation (7) to determine the radius of the laminar liquid jet. Test 63, which had both an 8-cm-long outlet tube and appreciable liquid depth at a jet Reynolds number of 1850, was observed to have a completely turbulent liquid jet.

Tests 38, 45, and 69 were all conducted under normal-gravity conditions with liquid depths over the liquid-jet outlet tube of approximately 2.5 cm and jet Reynolds numbers that ranged from 900 to 5150. For these test conditions the geysers that formed had the appearance of a "fountain" with no distinct liquid-vapor interface (footnote a in table I), and the incoming liquid fell back into the bulk-liquid region, causing centralized mixing only.

At the highest liquid-jet flow rates tested, Reynolds numbers of approximately 7500, undesirable liquid flow characteristics resulted under both zero- and normal-gravity conditions (tests 46, 48, and 49). Under zero-gravity conditions the liquid flow down the tank walls was entrained by the liquid jet so that most of the dyed liquid recirculated in the vapor region of the tank and very little bulk-liquid mixing resulted (footnote b in table I). For all three tests these high liquid-jet flow rates caused bubbles to be entrained in the bulk liquid (footnote c in table I) and thus defeated the objective of providing bulk liquid of uniform temperature and density.

Spherical tank tests 81 and 83, conducted under zero-gravity conditions with liquid fillings of approximately 70 percent, exhibited bulk-liquid collection on the sides of the container after the start of liquid-jet flow. The jet liquid passed through the central portion of the container and flowed over the bulk liquid to the bottom of the tank (footnote d in table I); no bulk-liquid mixing resulted. At experimental conditions of zero gravity and approximately 90 percent liquid filling of the spherical tank (tests 87 and 89), the start of liquid-jet flow caused the bulk liquid to collect at the end of the tank opposite the jet exit and the vapor bubble to be drawn into the simulated mixer inlet (footnote e in table I).

The author anticipated that the application of a small acceleration would be sufficient to position the bulk liquid positively and thus to avoid the just discussed problems associated with relatively high liquid fillings in spherical tanks. In general, the stabilizing influence of a small acceleration did in fact lead to desirable liquid flow patterns and uniform mixing of the liquid bulk. However, test 90 proved to be the exception that leads to the conclusion that axial liquid-jet mixing of propellants in spherical tanks will still be difficult even under reduced-gravity conditions. For this test, flow pattern IV was observed at a liquid filling of approximately 90 percent, but the bulk-liquid mixing was restricted to the central portion of the container (fig. 6).

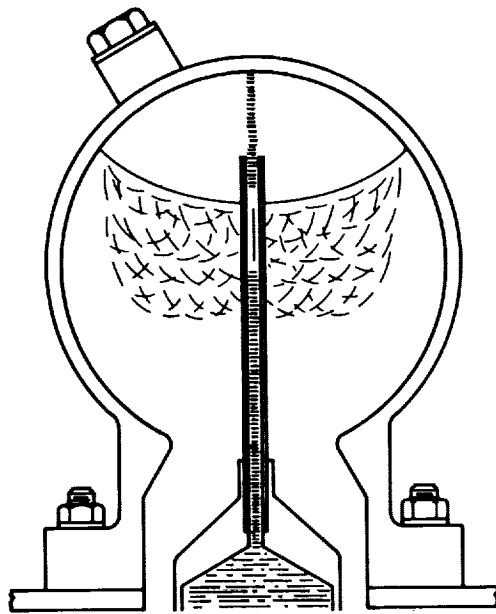


Figure 6. - Low-gravity bulk-liquid mixing, liquid filling, 90 percent, test 90.

Application of the cylindrical tank flow-characterization-parameter calculation procedure to the spherical tank data yielded less than satisfactory results. The calculated flow characterization parameters were consistently higher than the experimentally determined nondimensional geyser heights. Under zero- and reduced-gravity conditions the liquid-vapor interface has a smaller radius of curvature in spherical tanks than in cylindrical tanks because of the curvature of the tank wall. The author suggests that, because of this more highly curved liquid-vapor interface, the radius of the spherical tank is probably not an appropriate characteristic dimension to be used to nondimensionalize the geyser height. However, since the amount of spherical tank data was limited, no attempt was made to establish a more appropriate characteristic dimension or flow characterization parameters specifically for spherical tanks.

APPLICATION OF MODELING TECHNIQUE

To demonstrate the use of the correlations developed in the section Analysis of Experimental Results, a typical liquid-hydrogen tank and internal thermodynamic vent system designed for space operation have been analyzed. The selected propellant tank (ref. 14) and internal thermodynamic vent system (ref. 3) are for a shuttle-compatible space tug that is very similar to current orbit transfer vehicle concepts. Table II is a summary of the parameters used for this analysis and the resulting recommendations.

It was assumed that the liquid-hydrogen tank is covered with multilayer insulation (30 layers) so that the resulting in-space heating rate of approximately 88 W (300 Btu/hr) would match the cooling capability of the reference 3 thermodynamic vent system. At this design point the mixer unit provides a liquid-hydrogen flow rate of 2300 cm³/sec (1320 lb/hr) through the 4.4-cm (1.75-in.) diameter outlet tube. The corresponding overboard vent rate is 0.8 kg/hr (1.7 lb/hr). The electric power required for the mixer at this design point is approximately 7 W, with a resulting increase in the rate of heat addition to the tank contents of 2.3 W (8 Btu/hr).

TABLE II. - APPLICATION OF MODELING

TECHNIQUE PARAMETERS AND RESULTS

Liquid-hydrogen tank:	
Diameter, m(ft)	4.3 (14)
Length, m(ft)	6.1 (20)
Volume, m ³ (ft ³)	71 (2500)
Heating rate, W(Btu/hr)	88 (300)
Reference 3 mixer unit characteristics:	
Flow rate, cm ³ /sec(lb/hr)	2300 (1320)
Outlet tube diameter, cm(in.)	4.4 (1.75)
Cooling rate, W(Btu/hr)	88 (300)
Overboard vent rate, kg/hr(lb/hr)	0.8 (1.7)
Recommended mixer unit and resulting liquid-jet characteristics:	
Flow rate, cm ³ /sec(lb/hr)	3450 (1980)
Outlet tube diameter, cm(in.)	17 (6.7)
Cooling rate, W(Btu/hr)	132 (450)
Overboard vent rate, kg/hr(lb/hr)	1.2 (2.6)
Jet velocity, cm/sec(ft/sec)	15 (3.2)
Jet Weber number ^a	3.3 to 12.1
Jet Bond number ^a	0.85 to 0
Flow characterization parameter ^a	3.2 to 18.9

^aTank fillings range from 90 to 20 vol% and acceleration environment ranges from 3×10^{-6} g's to 0.

A typical multiburn orbit-raising mission was selected for the orbit transfer vehicle. Consequently the liquid-hydrogen propellant tank conditions varied from, initially, a nearly full tank in low Earth orbit with an acceleration level (caused by atmospheric drag) of approximately 3×10^{-6} g to, just before the final engine burn, a tank approximately 20 percent full and an acceleration level of essentially zero.

Because of the low viscosity of liquid hydrogen the liquid-jet Reynolds number is very high and equation (6) can be used to establish the radius of the completely turbulent liquid jet at the liquid-vapor interface. Weber numbers were calculated for a range of orbit transfer vehicle hydrogen-tank liquid fillings by using equation (3). At the mixer unit design-point flow rate of 2300 cm³/sec the liquid-jet Weber number exceeds 60 at low tank fillings. On the basis of model tank experimental data a submerged liquid-jet Weber number in excess of 30 indicates that turbulent, recirculating liquid flow plus the formation of bubbles will probably result - a highly undesirable situation.

Increasing the diameter of the liquid-jet outlet tube while maintaining the same mixer flow rate and thus the same heat-exchanger cooling capacity will reduce the liquid-jet Weber numbers to within acceptable limits. A liquid-jet outlet tube diameter of 17 cm (6.7 in.) was chosen to provide dimensional similitude with the model experiment tanks (tank diameter to jet outlet diameter ratio, 25). The liquid-jet Weber and Bond numbers were calculated by using equations (2) and (3) with a resulting maximum value for the Weber number of 5. The corresponding values of the flow characterization parameter varied from 1.2 to 7.5. Consequently, as the tank filling decreases during the mission, a transition from flow pattern II to flow pattern IV would occur - a highly undesirable situation.

To achieve dissipation of the liquid jet in the bulk-liquid region (flow pattern I), the flow characterization parameter should be less than 0.5. Obviously, for the orbit transfer vehicle chosen as an example, achieving

flow pattern I would be impossible without either using a very large-diameter jet outlet tube or reducing the liquid-jet flow rate and thus the cooling capacity of the thermodynamic vent system. Of more concern is the avoidance of flow patterns II and III and the resulting lack of bulk-liquid mixing. The author suggests that, in addition to using a 17-cm-diameter liquid-jet outlet tube, the jet flow rate should also be increased by approximately 50 percent. This higher liquid-jet flow rate will yield jet Weber numbers and flow characterization parameters that will guarantee complete liquid circulation (flow pattern IV) without the possibility of undesirable liquid flow conditions. In addition, the higher flow rate will provide additional thermodynamic vent system cooling capacity to allow for any uncertainty in the rate of heat input to the liquid-hydrogen tank.

Further examination of orbit transfer vehicle requirements reveals that the heating load on the liquid-hydrogen tank while it is still in the shuttle cargo bay may be as much as five times higher than the in-space heating load (ref. 15). This higher heat transfer rate results primarily from the time required for the multilayer insulation to become evacuated following exposure to the vacuum of space. If an internal thermodynamic vent system must provide liquid-hydrogen-tank pressure control while the orbit transfer vehicle is in the shuttle cargo bay, a much larger system than that reported on in reference 3 will be required. To accommodate the complete range of propellant tank conditions (heating rate, liquid filling, and acceleration environment), it may be necessary to design the thermodynamic vent system for both intermittent operation and variable mixer unit flow rate capability.

CONCLUDING REMARKS

Fluid Dynamic Analysis

The analytical technique of employing dimensional analysis to provide fluid dynamic criteria for the in-space operation of liquid-fueled propulsive stages is well established (ref. 16). Specifically, the use of the Bond and Weber number nondimensional parameters to establish the similarity between ground-based experimental programs conducted in drop towers using scale-model tanks and the in-space operation of full-scale vehicles has been demonstrated (ref. 17). This analytical technique has been applied to the problems of establishing the criteria for liquid-vapor interface stability, liquid reorientation, propellant tank draining, and liquid inflow to propellant tanks under reduced-gravity conditions.

The fluid dynamic analysis presented herein is a logical extension of the dimensional analysis technique to the problem of mixing propellants in space. For the cylindrical tank data an excellent correlation resulted between the experimentally determined nondimensional geyser heights and the newly defined flow characterization parameter (fig. 4). That this correlation was good over a wide range of liquid-jet flow conditions and gravitational environments lends credence to the use of this technique to predict axial liquid-jet flow patterns in full-scale propellant tanks.

Fluid Mixing Analysis

Liquid-jet mixing parameters have been shown to be a function of the jet Reynolds number under normal gravity (refs. 10 and 11). A previous attempt

(ref. 18) to correlate reduced- and normal-gravity liquid-jet mixing phenomena also used the jet Reynolds number to characterize the liquid jet. This approach led to vastly different values for the mixing parameters when experimental data with the same jet Reynolds number but different acceleration environments were compared.

The most significant contribution to liquid mixing theory reported herein is the establishment of flow characterization parameters that are functionally related to a simplified version of the Okita and Oyama mixing parameter (ref. 12) over a wide range of experimental conditions. Of particular importance is the fact that the range of acceleration environments explored covered several orders of magnitude.

The use of dyed ethanol to simulate the mixing of cryogenic propellants does, however, leave two unresolved issues: (1) how the mixing of dyed and undyed liquids is related to the mixing of liquids of different temperature; and (2) how the differences in fluid properties between ethanol and typical cryogenic propellants influence the mixing parameter. The correlation between the flow characterization parameters and the simplified Okita and Oyama mixing parameter that has been established suggests that future experimental data obtained under normal-gravity conditions can be used to resolve these issues and to predict the in-space performance of axial liquid-jet mixing devices.

SUMMARY OF RESULTS

An experimental program was conducted in the Lewis Research Center's zero-gravity facility to examine the liquid flow patterns that result from the axial jet mixing of ethanol in 10-cm-diameter containers under zero-, reduced-, and normal-gravity conditions. Four tank configurations were used for the study: a spherical container; a convex hemispherically ended cylindrical container; and two Centaur liquid-hydrogen-tank models, one with slosh baffles and one without.

How the gravitational environment, the tank configuration, the position of the liquid-jet outlet tube relative to the liquid-vapor interface, and the liquid-jet volumetric flow rate affected the liquid flow patterns was examined. Four distinct liquid flow patterns were observed:

- (1) Pattern I - dissipation of the liquid jet in the bulk-liquid region
- (2) Pattern II - geyser formation
- (3) Pattern III - collection of the jet liquid in the aft end of the tank (opposite jet outlet)
- (4) Pattern IV - liquid circulation over the aft end of the tank and down the tank wall

Nondimensional parameters (Reynolds, Weber, and Bond numbers) that are typically applied to the analysis of fluid dynamic phenomena were used to characterize the liquid jets and the resulting liquid flow patterns. The Reynolds number provides differentiation between the laminar, transition, and turbulent liquid-jet flow regimes. The experimentally observed geyser height, divided by the tank radius, was chosen to characterize the observed flow patterns. This nondimensional geyser height was correlated with a new nondimensional grouping of the Weber and Bond numbers (flow characterization parameters) in both the transition and turbulent liquid-jet flow regimes.

The liquid-bulk mixing phenomena, expressed as the ratio of liquid-jet volumetric flow rate to liquid-bulk mixing rate, for liquid flow patterns I and IV were shown to be a function of the flow characterization parameters over a wide range of experimental variables. Although a great deal of

scatter exists in the data, this mixing parameter also adds insight to the liquid-bulk mixing phenomenon for liquid flow pattern II. No liquid-bulk mixing occurs for liquid flow pattern III.

Use of the flow characterization parameters to determine mixer requirements for a full-scale orbit transfer vehicle (OTV) hydrogen tank yields the following conclusions:

1. A mixer designed to achieve dissipation of the liquid jet in the bulk-liquid region (flow pattern I) will require low liquid-jet flow rates and large heat exchangers.

2. The recommended mixer design is based on achieving complete liquid circulation (flow pattern IV) during the OTV orbit-raising mission.

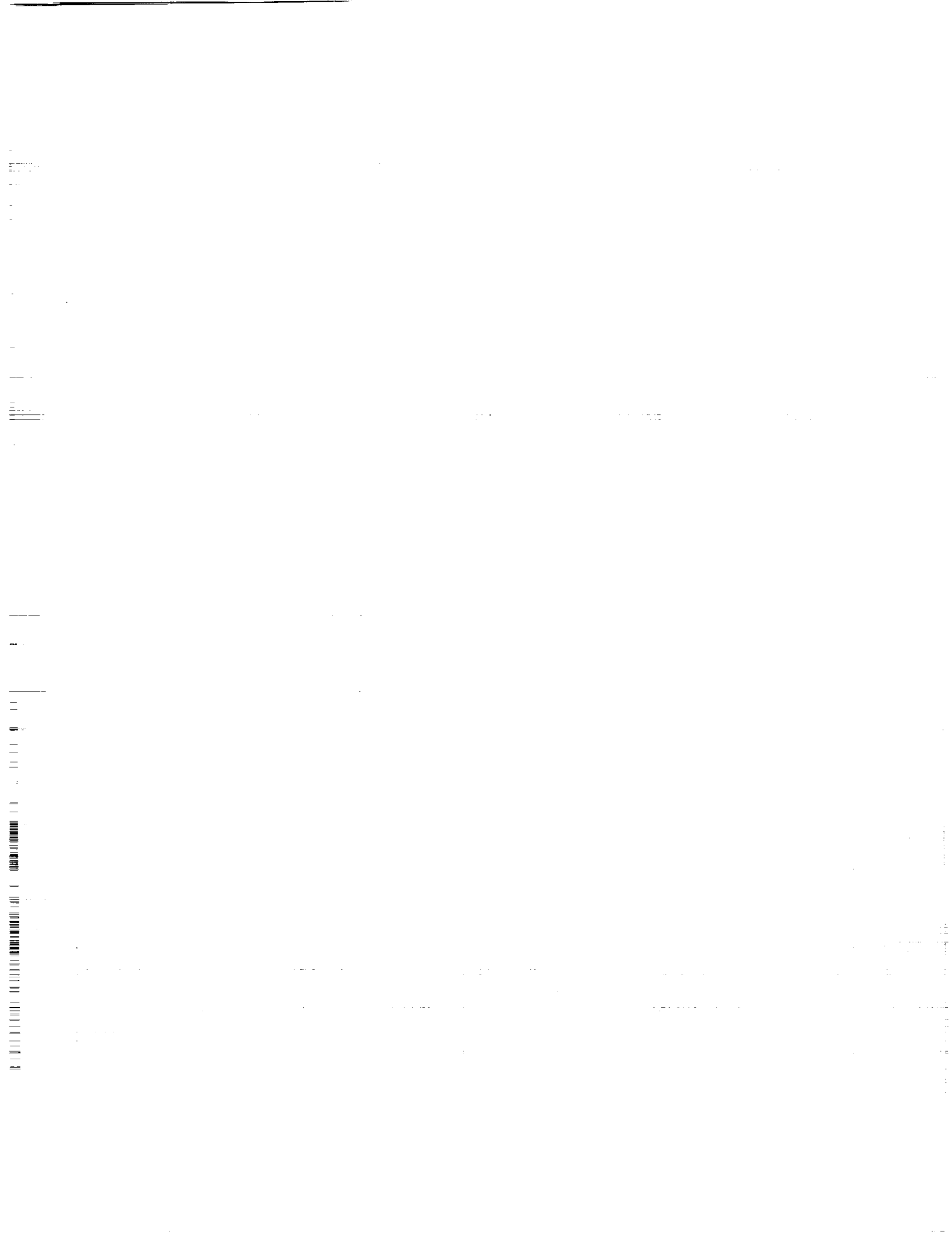
3. The anticipated variation in tank heating rates for cryogenic tankage transported to orbit by the shuttle may require multiple flow rate capability and/or periodic operation of the mixer unit.

Lewis Research Center
National Aeronautics and Space Administration
Cleveland, Ohio, July 2, 1982

REFERENCES

1. Lacovic, R. F.; et al.: Management of Cryogenic Propellants in a Full-Scale Orbiting Space Vehicle. NASA TN D-4571, 1968.
2. Stark, J. A.; and Blatt, M. H.: Cryogenic Zero Gravity Prototype Vent Systems. (GDC-DDB67-006, General Dynamics Convair; NASA Contract NAS8-20146.) NASA CR-98079, 1967.
3. Bullard, B. R.: Liquid Propellant Thermal Conditioning System Test Program. (LMSC-D159262, Lockheed Missiles and Space Co.; NASA Contract NAS3-12033.) NASA CR-72971, 1972.
4. Aydelott, J. C.: Axial Jet Mixing of Ethanol in Spherical Containers During Weightlessness. NASA TM X-3380, 1976.
5. Aydelott, J. C.: Axial Jet Mixing of Ethanol in Cylindrical Containers During Weightlessness. NASA TP-1487, 1979.
6. Symons, E. P.; and Staskus, J. V.: Interface Stability During Liquid Inflow to Partially Full, Hemispherical-Ended Cylinders During Weightlessness. NASA TM X-2348, 1971.
7. Spuckler, C. M.: Liquid Inflow to Initially Empty Cylindrical Tanks in Low Gravity. NASA TM X-2613, 1972.
8. Albertson, M. L.; et al.: Diffusion of Submerged Jets. Am. Soc. Civil Eng., Proc., vol. 74, no. 10, Dec. 1948, pp. 1571-1596.
9. Schlichting, Hermann (J. Kestin, transl.): Boundary Layer Theory. Sixth ed. McGraw-Hill Book Co., Inc., 1968.

10. Drew, T. B.; Hooper, J. W., Jr.; and Vermeulen, T.: Advances in Chemical Engineering, Vol. 3. Academic Press Inc., 1962.
11. Uram, E. M.; and Goldschmidt, V. W.: Fluid Mechanics of Mixing. ASME, 1973.
12. Okita, N.; and Oyama, Y.: Mixing Characteristics in Jet Mixing. Chem. Eng. Jpn., vol. 1, no. 1, 1963, pp. 94-101.
13. Schach, W.: Deflection of a Free Fluid Jet at a Flat Panel. NASA Technical Translation F-15151, Oct. 1973.
14. Blatt, M. H.; Bradshaw, R. D.; and Risberg, J. A.: Capillary Acquisition Devices for High Performance Vehicles - Executive Summary. (GDC-CRAD-80-003, General Dynamics/Convair; NASA Contract NAS3-20092.) NASA CR-159658, 1980.
15. Sumner, I. E.: Thermal Performance of a Gaseous-He-Purged Tank-Mounted Multilayer Insulation System During Ground-Hold and Space-Hold Thermal Cycling and Exposure to Water Vapor. NASA TP-1114, 1978.
16. Aydelott, J. C.; and Symons, E. P.: Lewis Research Center Reduced Gravity Fluid Management Technology Program. NASA TM-81450, 1980.
17. Lacovic, R. F.: Centaur Zero Gravity Coast and Engine Restart Demonstration on the Titan/Centaur (TC-2) Extended Mission. NASA TM X-71821, 1975.
18. Blatt, M. H.; Pleasant, R. L.; and Erickson, R. C.: Centaur Propellant Thermal Conditioning Study. (CASD-NAS-76-026, General Dynamics/Convair; NASA Contract NAS3-19693.) NASA CR-135032, 1976.



1. Report No. NASA TP-2107	2. Government Accession No.	3. Recipient's Catalog No.	
4. Title and Subtitle MODELING OF SPACE VEHICLE PROPELLANT MIXING		5. Report Date January 1983	6. Performing Organization Code 506-52-42
		7. Author(s) John C. Aydelott	8. Performing Organization Report No. E-1275
9. Performing Organization Name and Address National Aeronautics and Space Administration Lewis Research Center Cleveland, Ohio 44135		10. Work Unit No.	11. Contract or Grant No.
		13. Type of Report and Period Covered Technical Paper	
12. Sponsoring Agency Name and Address National Aeronautics and Space Administration Washington, D. C. 20546		14. Sponsoring Agency Code	
		15. Supplementary Notes	
16. Abstract An experimental program was conducted to examine the liquid flow patterns that result from the axial-jet mixing of ethanol in 10-cm-diameter spherical and cylindrical containers under zero-, reduced-, and normal-gravity conditions. Dimensionless parameters were developed that characterized the observed liquid flow patterns and the bulk-liquid mixing phenomena.			
17. Key Words (Suggested by Author(s)) Liquid propellants; Fluid dynamics; Axial liquid jet; Mixing; Reduced gravity; Dimensional analysis		18. Distribution Statement Unclassified - unlimited STAR Category 28	
19. Security Classif. (of this report) Unclassified	20. Security Classif. (of this page) Unclassified	21. No. of Pages 27	22. Price* A03